

MicroRNA-365 targets multiple oncogenes to inhibit proliferation, invasion, and self-renewal of aggressive endometrial cancer cells

Chunfang Wang
Ke Su
Yanyan Zhang
Weiwei Zhang
Danxia Chu
Qian Zhao
Ruixia Guo

Department of Gynecology, The First
Affiliated Hospital of Zhengzhou
University, Zhengzhou, Henan 450052,
China

Background: MicroRNA-365 (miR-365) has been reported to be a tumor suppressor miRNA. However, the role of miR-365 in progression of endometrial cancer (EC) has not been explored, in this study, we have found that re-expression of miR-365 inhibits cell proliferation, causes apoptosis and senescence.

Materials and methods: Overexpression of miR-365 attenuated cell migration and invasion, inhibited sphere-forming capacity and enhanced the chemosensitivity to paclitaxel. In silico prediction tools identified the potential targets of miR-365.

Results: We identified *EZH2* and *FOS* as targets of miR-365 and found that downregulating these genes imitated the tumor suppressive effect of miR-365. The outcomes of the study suggested that a reverse correlation existed between low miR-365 and overexpression of *FOS* and *EZH2* in EC tissue specimens.

Conclusion: The study indicates that miR-365 acts as an important tumor suppressor and contributes by suppressing cell invasiveness, proliferation, and self-renewal in cancer cell lines by regulating multiple oncogenes. We establish that miR-365-EZH2/FOS pathway is an important target for treating EC.

Keywords: microRNA-365, endometrial cancer, paclitaxel, *EZH2*, *FOS*

Introduction

MicroRNAs, also called as miRs, are short non-coding RNAs which alter the levels of a number of protein-coding mRNAs via degrading mRNA or by suppressing their translation.¹ They are reported to regulate a number of cellular processes, among which apoptosis, proliferation, and differentiation are the major ones; thus, any deregulation leads to development of tumors and their metastasis.²⁻⁵ Some miRNAs are identified to induce certain types of cancers, contributing to development of specific tumors.⁶ Some miRNAs, such as miR365, have been identified to act as tumor suppressors or oncogenes in a number of cancers. It has been found that miR365 regulates lung cancer and developmental gene thyroid transcription factor 1,⁷ induces cutaneous squamous cell carcinoma,^{8,9} induces gemcitabine resistance in pancreatic cancer cells,¹⁰ contributes to gastric tumorigenesis,¹¹ halts breast cancer cell growth, induces chemoresistance via GALNT4 pathway,¹² and inhibits malignant melanoma, colon cancer, and ovarian cancer.¹³⁻¹⁵

Endometrial carcinoma (EC) is reported to be one of the most common gynecological malignancies; it is classified into two types called as type I and type II EC.¹⁶ Type I is common, occurring in ~85% cases, and is characterized by the presence of

Correspondence: Ruixia Guo
Department of Gynecology, The
First Affiliated Hospital of Zhengzhou
University, Zhengzhou, Henan 450052,
China
Tel +86 13 5255 69376
Email 1747583701@qq.com

well-differentiated tumors of low grade and good prognosis. In type II EC, clear cell carcinoma is present, which arises in atrophic endometrium. Type II is an aggressive form of EC, which shows tumors that are not well differentiated and are of high grade and poor prognosis. Type II EC is uncommon and accounts for ~15% of all EC cases; however, it is awful and accounts for 50% of all relapses of EC.¹⁷ Thus, identifying the molecular mechanism of growth and advancement of aggressive EC would be practicable in designing therapeutic and diagnostic approaches for bettering the survival of EC patients.

In EC, literatures have confirmed involvement of miRNAs such as miR-449, miR-106a, miR-let7c, miR-185, miR-205, miR-423, miR-107, miR-181a, miR-429, miR-210, and miR-103 in oncogenesis, invasion, and metastasis of EC.^{18–20} So far, a number of pathways have been found to be involved in EC; for instance, overexpression of miR-200b in adenocarcinoma cells caused inhibition of tissue inhibitor of metalloproteinase (TIMP)-2 and elevated the expression of matrix metalloproteinase, that is, MMP-2.²¹ Reports have confirmed that downregulation of miR-let7e, miR-221, miR-193, miR-152, miR-30c, miR-99b, miR-204, and miR-193b halts the process of oncogenesis, invasion, and metastasis in EC.^{18–20}

Among various miRNAs, miR-125b has been identified to act as an oncogene by promoting the proliferation of EC cell lines both in vivo and in vitro.²² Some of the miRNAs such as miR-34,²³ miR-194,²⁴ and miR-106b²⁵ are found to be downregulated in EC. miR365 has recently been identified to act as an inhibitor in some malignancies. For instance, overexpression of miR-365 has been found to inhibit breast cancer both in vitro and in vivo,¹⁵ miR365 suppresses tumor proliferation and metastasis in malignant myelomas,^{13,26} miR365 has been found to target NF- κ B to inhibit squamous cell carcinoma,²⁷ and also, a study concluded the role of miR-365 in the regulation of myelin D in inhibiting the proliferation of smooth muscle cells.²⁸ Although there are many evidences suggesting the tumor suppressor role of miR-365 in cancer, a study suggests miR365 acts as an oncogene in cutaneous squamous cell carcinoma.³⁰ Looking into the possibility that miR365 shows dual role in various malignancies, the role of miR365 in tumorigenesis, its biological function, and its actual target in aggressive EC are unexplored.

Here, we report that miR365 targets multiple oncogenes such as FOS, EZH2, and MCL-1 and inhibits proliferation, invasion, and self renewal of aggressive EC cells. We also found that suppression in the expression of miR-365 was inversely related to the expression levels of FOS, EZH2, and MCL-1 in EC-affected tissues.

Materials and methods

EC cell lines and cell transfection

For the study, human EC SPAC-1-S and -1-L cell lines were selected and obtained from the Department of Gynecology, The First Affiliated Hospital of Zhengzhou University, China. For the use of the cell lines, ethical clearance was obtained from the institutional review board of The First Affiliated Hospital of Zhengzhou University. The cells were stored using RPMI-1640 medium (Thermo Fisher Scientific, Waltham, MA, USA) along with fetal bovine serum (FBS) 10%. An immortal strain of human endometrial epithelial cells, that is, the EME cell lines, was obtained from the Department of Gynecology. The HOTA-1 and HEC-155 cell lines were isolated from endometrioid, followed by multiplication in a DMEM/F12 medium along with FBS (10%).

The process of transfection in cell was done using Lipofectamine 2000 reagent (Thermo Fisher Scientific) in accordance with the manufacturer's instructions. The miR365, negative control (NC), miR-365-specific inhibitor (AS-365), anti-miRNA NC, small interfering RNA-EZH2 (siEZH2), small interfering RNA-FOS (siFOS), small interfering RNA-MCL-1 (siMCL-1), and the NC (siNC) were procured from Ambion (Austin, TX, USA). The transfection was done using miRNA (40 nM) and siRNA (10 nM).

Transfection of SPAC-L cells was done with pCMV-365 vector carrying pre-miRNA-365-3 p and pCMV-NC (ie, control vector) using Lipofectamine PLUS Reagent (Thermo Fisher Scientific).²⁷ The cells after transfection were selected using the selection antibiotic Geneticin (G418; 400 μ g/mL; Invivogen, San Diego, CA, USA). Six weeks following transfection, single cell colonies were selected.

Quantitative real-time reverse transcriptase-polymerase chain reaction (qRT-PCR) studies

For the qRT-PCR studies, total RNA was isolated from the cultured cells with the help of miRN easy mini kit (Qiagen, Hilden, Germany). The cDNA was primed at random using total RNA (2 μ g) with the Omniscript reverse transcription kit (Qiagen). The qRT-PCR study was done opting a dilution of 1:4 with cDNA using QuantiTect SYBR Green PCR kit using a QuantiTect SYBR Green PCR system (Qiagen). The forward primers required for the study were procured from Qiagen. The expression of mRNA was analyzed using 2^{- $\Delta\Delta$ Ct} method; actin was used for normalization, followed by comparison with controls.

The cell viability, colony formation, and proliferation assay

The cell viability assay was done using Cell Counting Kit-8 (Sigma-Aldrich Co., St Louis, MO, USA) in accordance with the manufacturer's protocol. Briefly, 5×10^3 cells were seeded in 96-well plates for 24 hours followed by exposure to paclitaxel of varying concentrations and dimethyl sulfoxide. The absorbance readings were recorded with the help of a microplate reader at 450 nm. The cell viability was calculated against readings of dimethyl sulfoxide-treated cell population. For colony formation assay, ~ 500 cells/well were seeded in six-well plates; the cells were cultured for 12 days at 37°C and fixed with formalin (10%) followed by staining with 10% Giemsa solution. The cell count was done using a microscope, number of cell colonies containing ≥ 50 cells were considered for the study, the count was done using a microscope. For cell proliferation studies, 2.5×10^3 cells were seeded in 96-well plates followed by transfection with miR-365 or NC as described earlier. The growth curves were plotted after analyzing 4 days of culture.

Cell invasion and migration assay

Cell invasion assay was performed using Transwell permeable supports (BD Biosciences, San Jose, CA, USA) following manufacturer's instructions. Briefly, to the upper insert of Transwell-permeable supports, 5×10^4 cells were added; serum-free medium was used to suspend the cells. To the lower chamber was added 750 μL of chemottractant medium (10% FBS). The cells were incubated for 24 hours. Cells adhered to the lower surface of the membrane, which were enumerated using an optical microscope. Cell migration assay was performed on a Transwell-permeable support with the membrane having Matrigel-coated polycarbonate. For the same, 5×10^4 cells were suspended in medium (serum free) and added to the lower chamber along with 750 μL medium, followed by incubation for 12 hours. Wound healing assay was done to evaluate cell migration. For this, the confluent cells were scraped to create an artificial wound, followed by incubation in mitomycin C-containing medium (5 $\mu\text{g}/\text{mL}$) for 12 hours. The distance traveled or migrated by cells was recorded by recording photographs at 0–12 hours.

Terminal deoxynucleotidyl transferase mediated dUTP nick-end labeling (TUNEL) assay (apoptosis studies)

TUNEL assay was done for determining apoptosis (Abcam, Cambridge, MA, USA) in accordance with the manufacturer's protocol. The MBT-2 cells were transfected with miR-365

vector as discussed earlier. After 72 hours, the cells were fixed, exposed to proteinase K, and then incubated with TdT reaction mixture. The MBT-2 cells were incubated along with streptavidin-HRP, after which color was developed with diaminobenzidine. The nuclei of cells that had undergone apoptosis were stained dark brown, showing the presence of fragmented DNA. The percentage of apoptotic cells in the total number of cells was calculated in four identified fields at $200\times$.

Enzymatic activity of caspase-3/-7

As a marker of apoptosis, the activities of both caspase-3 and caspase-7 were measured using caspase (3/7) assay kit (Promega Corporation, Fitchburg, WI, USA) following manufacturer's protocol. Briefly, 5×10^3 cells were transferred to 96-well plates followed by transfection as discussed earlier. The enzymatic activities of both caspase-3 and caspase-7 were measured by recording luminescence after 3 hours of incubation along with caspase substrate.

Senescence activity (senescence-associated β -galactosidase [SA- β -gal] staining)

As a marker of cellular senescence, the SA- β -gal activity was estimated using Senescence Assay Kit (Sigma-Aldrich Co.) following manufacturer's protocol. The cells were transfected as described earlier. After 72 hours, the transfected cells received PBS wash, following which they were treated with fixing solution and incubated for 15 minutes at room temperature conditions. The cells were washed after the fixing solution was removed using PBS, followed by incubation at 37°C for 12 hours along with 1X SA- β -gal detection solution in CO_2 -free conditions in the dark. The cells stained blue, indicating they were SA- β -gal positive, were counted and the percentage was calculated by counting about 200–250 cells in six randomly selected fields.

Immunoblotting studies

The cell lysates were collected using lysis reagent for Mammalian Protein Extraction (Thermo Fisher Scientific). A nuclear extraction kit was used to obtain nuclear extracts (Sigma-Aldrich Co.) following the manufacturer's instructions. The separation of proteins (nuclear proteins 10 μg and total proteins 40 μg) was done on sodium dodecyl sulfate-polyacrylamide gel electrophoresis (10%) followed by transfer to membranes of nitrocellulose. The generated antigen-antibody reaction complexes were observed by enhanced chemiluminescence technique.

The antibodies selected for the study were anti-PARP, anti-EZH2, rabbit polyclonal anti-E-cadherin, rabbit polyclonal anti-Vimentin, mouse monoclonal anti-N-cadherin, anti-MCL-1, anti-p21, anti-FOS, anti-Bax, anti-GAPDH, and anti- β -catenin. All the antibodies were obtained from Sigma-Aldrich Co. and Santa Cruz Biotechnology Inc. (Dallas, TX, USA). GAPDH and lamin B were selected as indicators for equal protein loading in whole cell lysates and nuclear protein extracts, respectively.

Sphere culture assay

For the sphere formation assay, HEC-50 and the SPAC-1-L (1,000 cells/mL) were cultured for 14 days in serum-free medium, which was supplemented with basic fibroblast growth factor (20 ng/mL), N2 supplement, epidermal growth factor (20 ng/mL), and 4 mg/mL heparin (Thermo Fisher Scientific). The criterion for counting was that spheres equal to or larger than 50 μ m were considered.

Microarray analysis

The transfection of cells was done as described earlier using pre-365 and NC. After 72 hours, Trizol reagent was used for isolating total RNAs. The expression of gene was analyzed with the help of Superprint G3 Human GE microarray (Agilent Technologies, Santa Clara, CA, USA).

3'-Untranslated region (UTR) dual-luciferase reporter assay

The Luciferase reporter vector of EZH2 and FOS were obtained from OriGene Technologies (Rockville, MD, USA). The human MCL-1 3'-UTR was procured from ABM Biotech. (Richmond, BC, Canada). Phusion Site-Directed Mutagenesis Kit (Thermo Fisher Scientific) was used for site-directed mutagenesis of miR-365 at the target site in MCL-1 3'-UTR. The cells were transferred into 24-well plates, followed by transfection with mutated vectors or wild-type miR-365, AS-miR-365, or NC. After 24 hours, the cells were collected and luciferase assay was performed by dual-luciferase reporter assay system. Luciferase Assay Reagent (Promega Corporation) was used to examine the effect of miR-365 on MCL-1 3'-UTR.

Human EC tissue samples and immunohistochemistry studies

The study protocol received ethical clearance from the human ethics committee of The First Affiliated Hospital of Zhengzhou University, China. Prior to study entry, written informed consent was signed by all the patients. For the study, EC tissues were collected from 40 subjects of grade

3 surgical resection at the Department of Gynecology, the First Affiliated Hospital of Zhengzhou University Hospital. In the study, ten endometrial specimens of normal tissues were considered as the normal comparative group. The tissue samples were fixed and embedded in paraffin blocks to obtain sections; also, about 12 pairs of endometrioid ECs and normal tissues adjacent to EC were collected. The tissue sections were evaluated for the expression levels of miR-365, FOS, and EZH2. The staining of tissue sections was done by streptavidin-biotin-peroxidase complex technique. The primary antibodies used for the study were FOS and EZH2, progesterone receptor (PR), and estrogen receptor (ER). The percentage positive (PT) cells and the mean staining intensity (SI) were considered for the expression of FOS and EZH2. The SI score was described as 0 for absence of staining, 1 was considered as weak staining, 2 as moderately stained, and 3 for strong staining. For the PT score, the criteria were fixed as: 0 for PT cells ranging from 0%–25%, 1 for 26%–50%, 2 for 51%–75%, and 3 for cells ranging from 76% to 100%. The score of immunostaining (IRS) was obtained by adding SI and PT. The IRS score graded the tumors based on rules established earlier.³² The IRS score was negative if it ranged from 0 to 2 and positive if it ranged from 3 to 7. The tumors showing ER/PR values >10% were considered as ER/PR positive.

Statistical analysis

All protocols in the study were done in triplicate. The values for in vitro experiments were expressed as average \pm standard error. The significance of results was established by performing either Student's *t*-test or Wilcoxon matched-pairs test, whereas Fisher's test was employed to equate the categorical data. The values of *P* < 0.05 were considered significant.

Results

miR-365 is downregulated in EC cell lines and regulates proliferation

To evaluate the involvement of miR-365 in EC cells, we compared the expression levels of miR-365 in four of the selected EC cell lines named HEC-155, HOUA-I, SPAC-1-L, and SPAC-1-S against immortalized epithelial cells of human endometrium. The results of qRT-PCR study suggested negative regulation of miR-365 in all the selected EC cells; highest downregulation was observed in both the SPAC-1-L and SPAC-1-S cells (Figure 1A), confirming miR-365 as a tumor suppressor in EC.

The effect of miR-365 transfection was studied on proliferation of EC cells. We found that the levels of miR-365 can

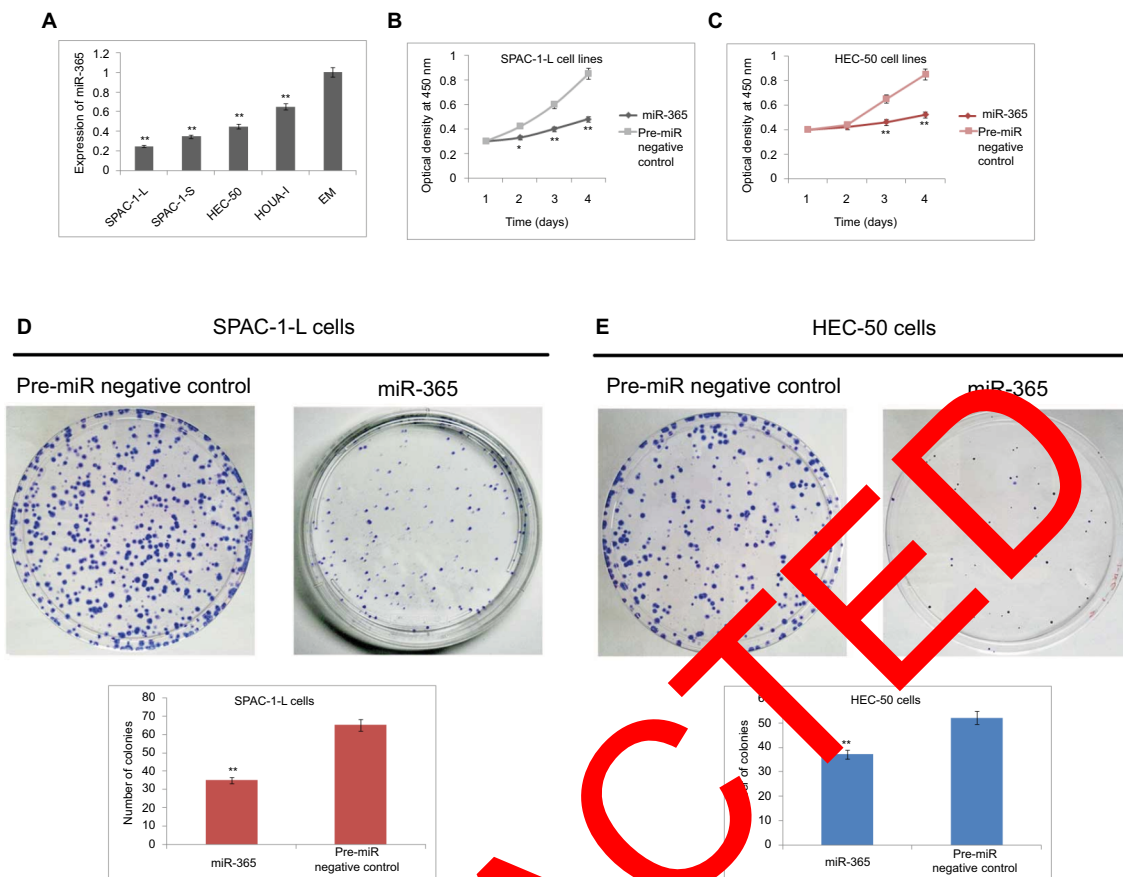


Figure 1 MiR-365 is down regulated in endometrial cancer cell lines and decreases cell proliferation

Note: (A) The qRT-PCR analysis was done for relative expression of miR-365 in 4 selected aggressive cancer cell lines along with immortalized EM cell lines. GAPDH was selected as loading control, the result are depicted as expression change against EM cells. (B and C) Results of cell counting kit for expression of miR-365 on proliferation of SPAC-1-L and HEC-50 cells against pre-miRNA negative control (NC)-transfected cells (* $P < 0.05$, ** $P < 0.01$). (D) Results of clone formation assay done on SPAC-1-L cells; (E) HEC-50 cells, transfected with pre-miR Negative control and pre-miR-365.

Abbreviations: NC, negative control; qRT-PCR, quantitative real-time reverse transcriptase-polymerase chain reaction.

be increased in the pre-miR-365-transfected SPAC-1-L cells by at least sixfold and in HEC-50 cells by fivefold, compared to normal control transfected cells. The results of transfection on cell proliferation were done using Cell Counting Kit-8. The results suggested that increasing the re-expression of miR-365 caused suppression of cell proliferation after 72 and 96 hours of transfection (Figure 1B, C). Further, colony formation assay was done on miR-365/NC-transfected SPAC-1-L and HEC-155 cells. As anticipated, the upregulation of miR-365 caused significant suppression of colony forming ability of both the cell lines (Figure 1D, E).

To figure out the involvement of apoptosis in reduction of cell proliferation due to transfection of miR-365, we performed the TUNEL staining assay of fragments of nuclear DNA. In the experiment, the DNase-treated SPAC-1-L cells and positive control cells showed positive TUNEL labeling.

The miR-365-transfected HEC-155 cells and SPAC-1-L cells showed higher number of apoptotic cells with brown-stained nucleus compared to control (Figure 2A, B). Further, the results of caspase-3 and caspase-7 suggested increased activity in miR-365-transfected cells compared to NC (Figure 2C).

In a direction to find the antiproliferative impression of miR-365, it was studied whether overexpression of miR-365 resulted in decreased proliferation due to cellular senescence. We subjected miR-365-transfected or NC HEC-155 and SPAC-1-L cells to SA- β -gal staining and morphology study 3 days post-transfection. The results suggested that miR-365 transfection resulted in cell enlargement and flattening along with positive staining for SA- β -gal (Figure 2D, E). The outcomes of Western blot suggested that overexpression of miR-365 resulted in increased expression of proapoptotic gene, that is, Bax, cleaved-PARP, an apoptosis marker, and p21,

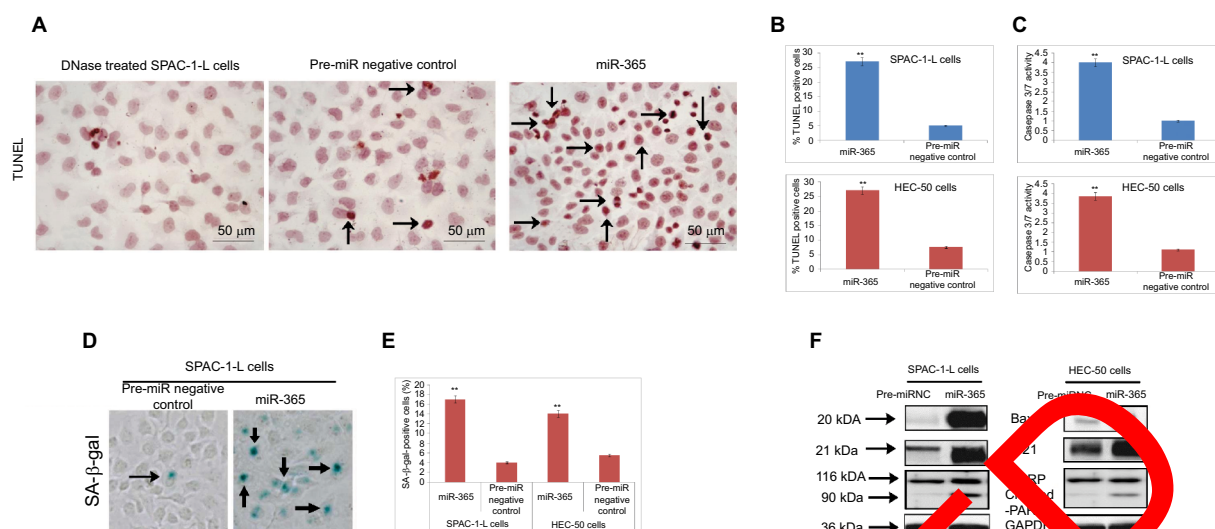


Figure 2 MiR-365 results in apoptosis of endometrial cancer cells.

Notes: (A) TUNEL assay for SPAC-1-L cells after 72 hours of transfection; the arrows show TUNEL-positive cells. (B) The results showing % TUNEL-positive HEC-50 and SPAC-1-L cells. (C) The results of caspase-3 and caspase-7 activity in both HEC-50 and SPAC-1-L cells after transfection with miR-365 or pre-miR NC for 72 hours. (D) SA-β-gal staining studies for miR-365 or NC transfected SPAC-1-L cells after 72 hours of transfection; the blue-colored cells are positive for SA-β-gal staining. (E) The results indicating % of SA-β-gal-positive HEC-50 and SPAC-1-L cells. (F) Results of Western blot studies for PARP, Bax, and GAPDH in HEC-50 and SPAC-1-L cells after transfection with miR-365 or pre-miR NC. (** $P < 0.01$ compared to NC.)

Abbreviations: NC, negative control; SA-β-gal, senescence-associated β-galactosidase; TUNEL, terminal deoxynucleotidyl transferase mediated dUTP nick-end labeling.

a senescence marker in both the cell lines (Figure 2F). The results of the study suggested that miR-365 caused apoptosis, increased the cell migration ability significantly, and/or senescence, which in turn inhibited the proliferative property of EC cells.

miR-365 halts the migration, invasion, and epithelial–mesenchymal transition (EMT) of EC cells

We studied the effect of miR-365 on the invasion and migration of HOUA-I cells, which showed higher expression of miR-365, and also of HEC-50 and SPAC-1-L cells, which showed lower levels of miR-365. The overexpressing SPAC-1-L cells were established by transfecting them with miR-365 expression vector, then pCMV-365, followed by evaluation of miRNA levels with qRT-PCR analysis. The effect of transfection on cell migration in SPAC-1-L cells was determined by wound healing assay using mitomycin C, which is an antiproliferative agent. We found that the SPAC-1-L cell lines showing overexpression of pCMV-365 had diminished wound healing effect compared to cells transfected with pCMV-control vector (Figure 3A). Further, we studied whether downregulation of miR-365 would induce the migration of EC cell line. For confirming the same, the HOUA-I cells were exposed to miR-365-specific inhibitor to suppress the miR-365 activity. Results of Transwell chamber assay sug-

gested that inhibition of miR-365 by an miR-365-specific inhibitor increased the cell migration ability significantly, whereas the NC cells failed to show the same. The results of Matrigel invasion studies suggested that, transfecting the HEC-50 and SPAC-1-L cells with miR-365 caused reduction in invasion capacity of both the cell lines (Figure 3B). We next studied whether suppressing the expression of miR-365 in SPAC-1-L cells (having higher invasion and epithelial-like morphology) can lead to increase in mesenchymal features. We observed that inhibiting miR-365 in SPAC-1-L cells using an miR-365-specific inhibitor changed the cellular morphology toward a more mesenchymal phenotype and also increased cell invasion. In agreement with these results, blocking of miR-365 using an miR-365-specific inhibitor in HOUA-I cell lines resulted in invasiveness and cell scattering. The results of protein expression by Western blot analysis suggested that re-expression of miR-365 in EC SPAC-1-L cell lines was accompanied by downregulation of Vimentin and N-cadherin (mesenchymal markers) and upregulation of E-cadherin (epithelial marker). Similarly, in HOUA-I cell lines, loss of miR-365 expression caused a significant suppression of E-cadherin and increased levels of Vimentin and N-cadherin (Figure 3C). All the findings suggested that the abnormal expression of miR-365 can suppress the invasive capability as well as the mesenchymal phenotype of EC cells.

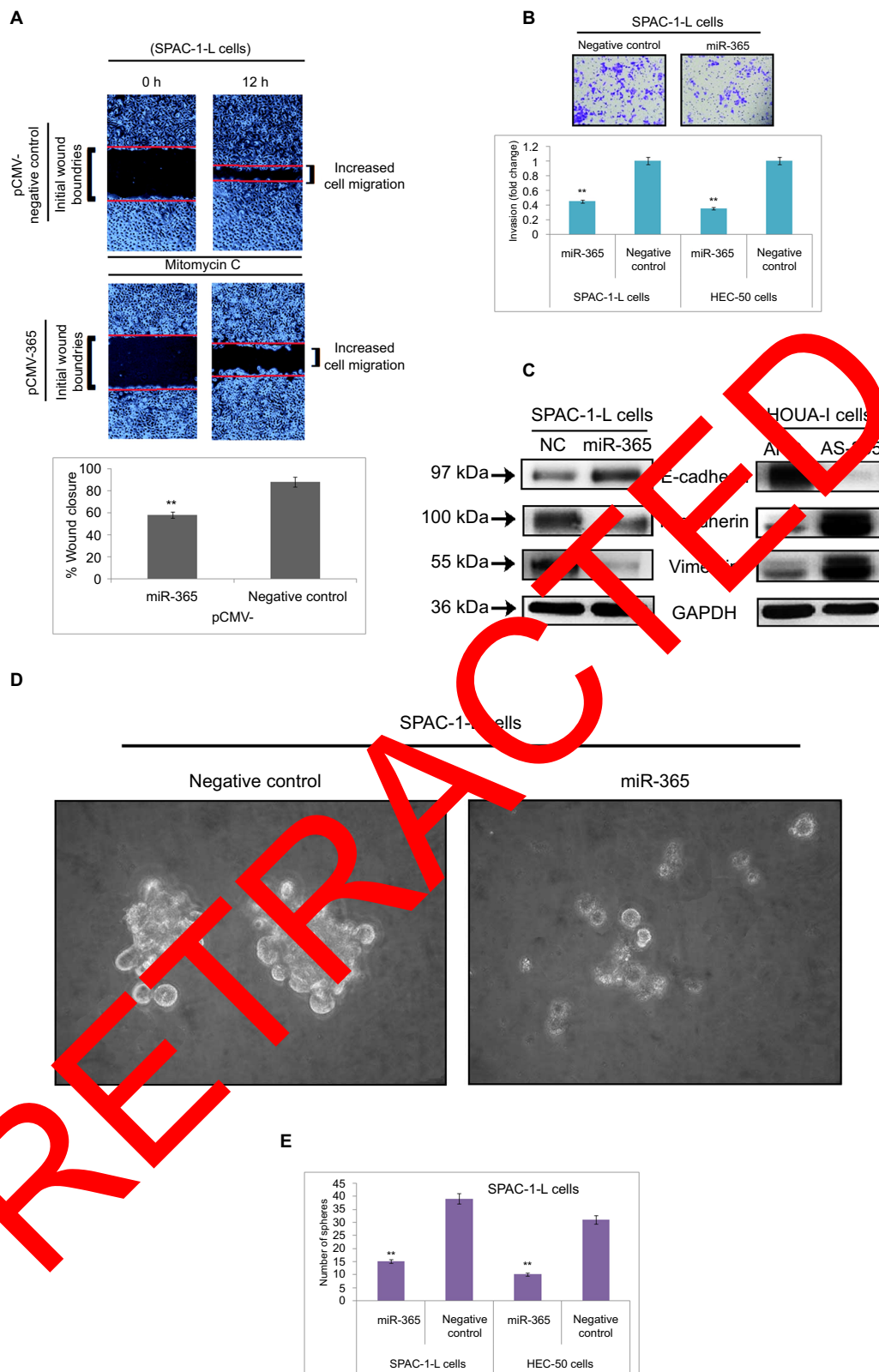


Figure 3 Over-expression of miR-365 inhibits cell migration and invasion in endometrial cancer cells.

Notes: (A) The results of scratch wound healing assay done in SPAC-1-L cells transfected with miR-365 or pre-miR NC along with mitomycin C. The extent of wound healing was identified at 0 and 12 hours; a visible increment was seen in cell migration compared to initial wound boundaries marked by red lines. The graph represents the % wound closure. (B) Results of cell invasion assay in HEC-50 and SPAC-1-L cells transfected with miR-365 or pre-miR NC. The images are from the membrane having cells. (C) Results of Western blot studies for the expression of Vimentin, N-cadherin, and E-cadherin in SPAC-1-L and HOUA-I cells after 72 hours of transfection with miR-365 or anti-miR-365 inhibitor (AS-365). (D) Images of sphere formation and (E) quantification results for sphere formation in HEC-50 and SPAC-1-L cells after transfection with miR-365. (** $P < 0.01$ compared to NC).

Abbreviation: NC, negative control.

The cancer cells have the property to acquire cancer stem cell (CSC)-like characteristics, which causes drug resistance, property to form mammospheres, and increases the levels of stem cell markers.^{30,31} In this study, we found that overexpression of miR-365 could lead to suppression of CSC-associated features. The results suggested that miR-365 transfection of SPAC-1-L cells caused decrease in the number of spheres in cultures (Figure 3D, E). Further, the results of cell counting assay suggested that overexpression of miR-365 caused increased sensitivity of SPAC-1-L cells against paclitaxel (Figure 4A), whereas downregulation of miR-365 suppressed the apoptotic property of paclitaxel in HOUA-I cells. Importantly, overexpression of miR-365 in SPAC-1-L caused decrease in the mRNA levels of *N-cadherin* and *Vimentin*, *ALDH*, *S100A4*, *NANOG*, *MDR1*, and *TWIST1*. The overexpression caused increased mRNA levels of *ZO-1*, *E-cadherin*,

desmoplakin, and *TIMP-3* (Figure 4B). The results further suggested that all these alterations were turned by silencing miR-365 in HOUA-I cells (Figure 4C). Altogether, the results of this experiment confirmed the suppressive role of miR-365 in EMT-mediated phenotypes of EC cells.

Identification of EZH2 and FOS as favorable target sites of miR-365

In silico analysis along with microarray gene expression was done in SPAC-1-L cells transfected with miR365 relative to the NC group of cells to confirm potential targets of miR-365. Prediction software “TargetScan” was used to identify conserved algorithm domain within 3'-UTR. About 12 genes were found to be targeted by miR-365 (Table 1). We further found the genes suppressed by overexpression of miR-365 in SPAC-1-L cells and identified *NEK7*, *UBE2D1*, and *FLRT3* as cancer-related



Figure 4 miR-365 enhances Paclitaxel sensitivity and suppresses EMT-mediated phenotypes of endometrial cancer cells

Notes: (A) Results of paclitaxel sensitivity in SPAC-1-L cells transfected with miR-365 or pre-miR negative control followed by treatment with paclitaxel for 24 hours. The results of cell viability are expressed as the % viable cells, considering 100% viability for DMSO-treated cells. (B, C) Results of relative mRNA expression of tumor cells undergoing EMT, invasion, and stemness-related genes in miR-365-overexpressing SPAC-1-L cells or in HOUA-I cells. GAPDH was used as the loading control. (** $P < 0.01$ compared to negative control.)

Abbreviations: AC, anti-miRNA negative control; DMSO, dimethyl sulfoxide; EMT, epithelial–mesenchymal transition.

genes (Table 1). The mRNA expressions of these three genes were suppressed by overexpression of miR-365 in SPAC-1-L cells and upregulated by a miR-365-specific inhibitor in HOUA-I cells (Figure 5A). In the study, we further found that *FOS* and

EZH2 were downregulated in miR-365-transfected SPAC-1-L cells (Figure 5B). In agreement with this, a negative correlation existed between miR-365 and the expression levels of *FOS* and *EZH2* in cells. We also established that transfection of miR-365 in SPAC-1-L cells caused suppression of expression of these genes, and that knockdown of miR-365 with miR-365-specific inhibitor resulted in upregulation of both *FOS* and *EZH2* in HOUA-I cells (Figure 5B, C).

The outcomes of luciferase activity suggested that exogenous miR-365 in SPAC-1-L cells suppressed the luciferase gene activity for mutation of *EZH2* 3'-UTR and *FOS* 3'-UTR (Figure 6A), whereas the miR-365-specific

Table 1 Twelve genes that were potential targets for miR-365 as predicted by TargetScan

miR-365 target genes (12)		
FLRT3	ZNF654	CDYL
GLTSCR1	MYCN	NEK7
ZCCHC2	FOS	FAM108C1
EYA1	RAP1B LRCH2	UBE2D1

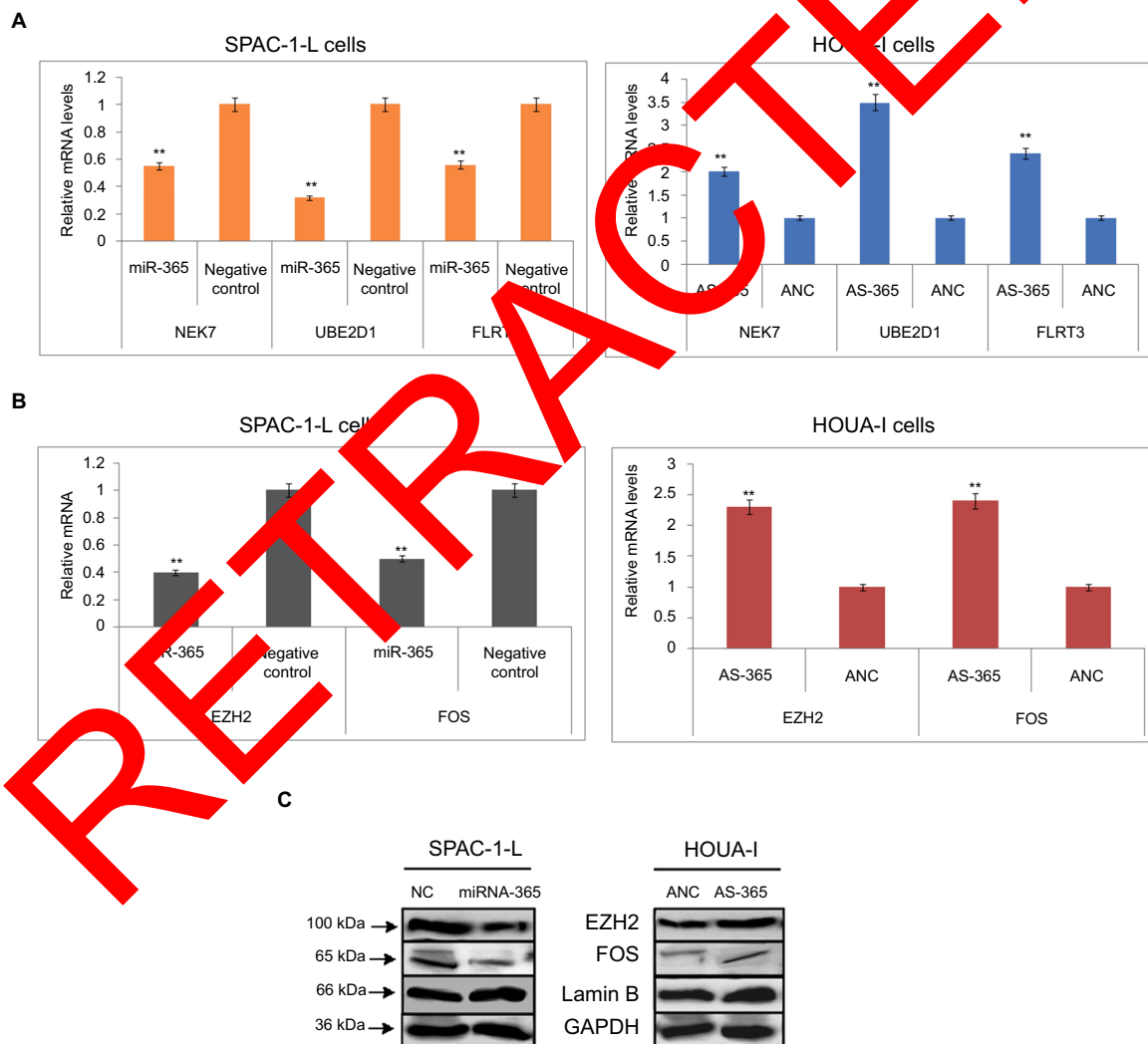


Figure 5 *EZH2* and *FOS* are direct targets of miR-365.

Notes: (A) Overexpression of miR-365 resulted in suppression of *FLRT3*, *NEK7*, and *UBE2D1* in SPAC-1-L cells, whereas suppression of miR-365 resulted in upregulation of these three genes in HOUA-I cells. (B) Overexpression of miR-365 resulted in suppression of *EZH2* and *FOS* in SPAC-1-L cells, whereas suppression of miR-365 caused upregulation of *EZH2* and *FOS* in HOUA-I cells. (C) Results of Western blot studies after transfection of SPAC-1-L cells with miR-365 on the levels of *EZH2* and *FOS* or with AS-365 in HOUA-I cells.

Abbreviations: ANC, anti-miRNA negative control; NC, negative control.

inhibitor in HOUA-I cells increased the luciferase activity (Figure 6A). On introduction of mutations into the 3'-UTR miR-365, the mutations for *EZH2* and *FOS* 3'-UTR forbade the suppression of activities by miR-365 (Figure 6B). All these in silico outcomes were affirmed in HOUA-I cells (Figure 6B), confirming that the restrictive effect of miR-365 was primarily due to its correlation with *EZH2* and *FOS* 3'-UTR.

Suppression of *EZH2* and *FOS* caused inhibition of invasion, CSC-like phenotype, and proliferation of EC cells

To identify whether knockdown of *FOS* and *EZH2* is a contributing factor for miR-365-mediated suppression of endometrial tumor, we suppressed these two genes with the help of siRNA in HEC-50 and SPAC-1-L cells. We found that suppression of these two genes (Figure 7A, B) caused apoptosis and senescence (Figure 8A, B) and may be a responsible factor for the inhibitory effect of *FOS* and *EZH2* siRNA on the proliferation of EC cells. We also discovered that, transfection of

FOS and *EZH2* siRNA in HEC-50 and SPAC-1-L cells caused a significant inhibition of their property to invade and form spheres, which imitated the tumor-suppressive effect after miR-365 overexpression. We also found that, the expression levels of mesenchymal markers such as nuclear β -catenin and Vimentin were significantly downregulated and the levels of epithelial markers such as proapoptosis factor Bax, p21, and E-cadherin were significantly upregulated after transfecting *FOS* and *EZH2* siRNA in both the cell lines (Figure 7A, B). The findings of protein expression suggested that suppression of *FOS* and *EZH2* oncogenes by miR-365 attenuated the invasion, proliferation, and CSC-like character of EC cells.

MiR-365 and its direct targets (*EZH2* and *FOS*) are inversely expressed in endometrial cancer tissues

In this study, we performed RT-PCR analysis for comparing the expression of *EZH2* and *FOS* along with miR-365 in EC tissues and normal tissues adjacent to them. We found

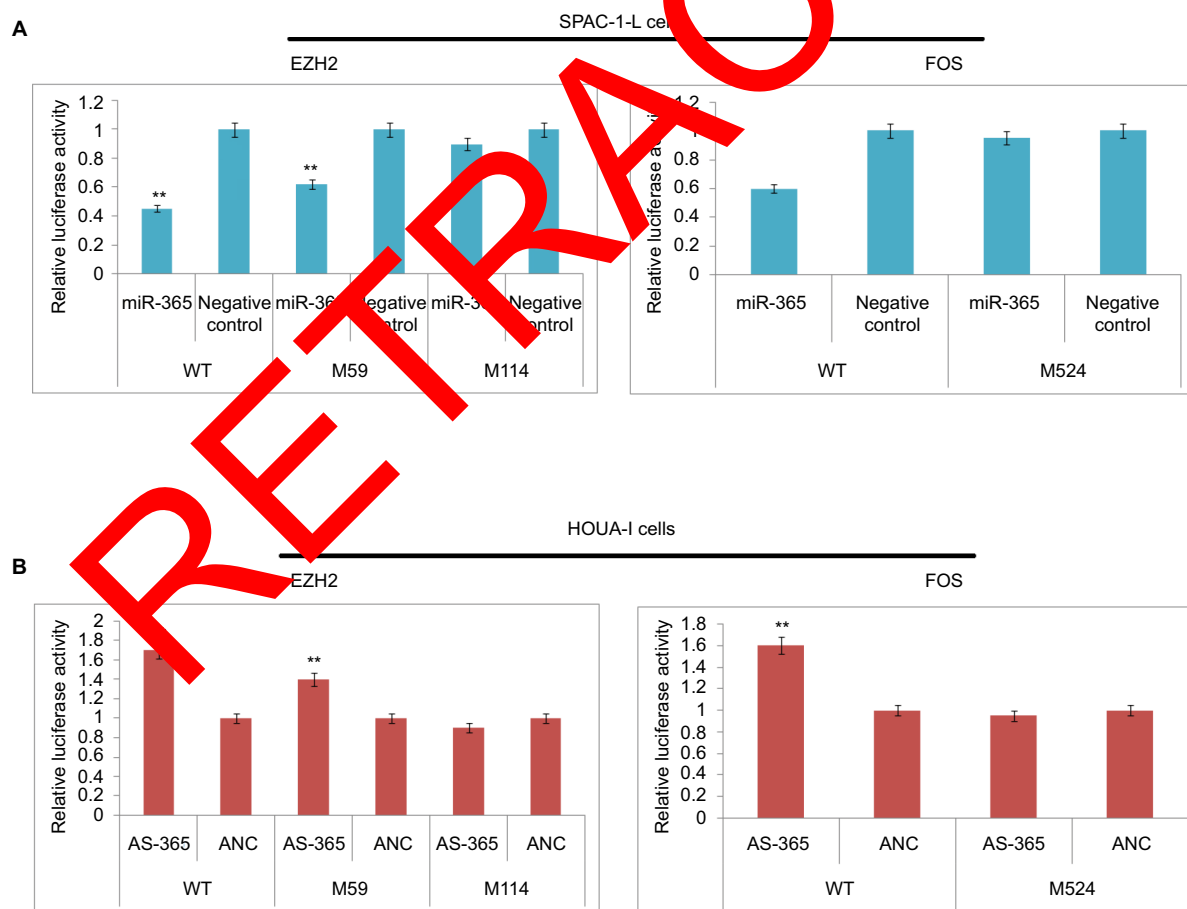


Figure 6 Luciferase study confirmed *EZH2* and *FOS* as direct targets of miR-365.

Notes: The luciferase reporter assays identified both *EZH2* and *FOS* as direct targets of miR-365 in both (A) SPAC-1-L and (B) HOUA-I cells. ** $P < 0.01$ compared to respective pre-miR negative control.

Abbreviations: ANC, anti-miRNA negative control; WT, wild type.

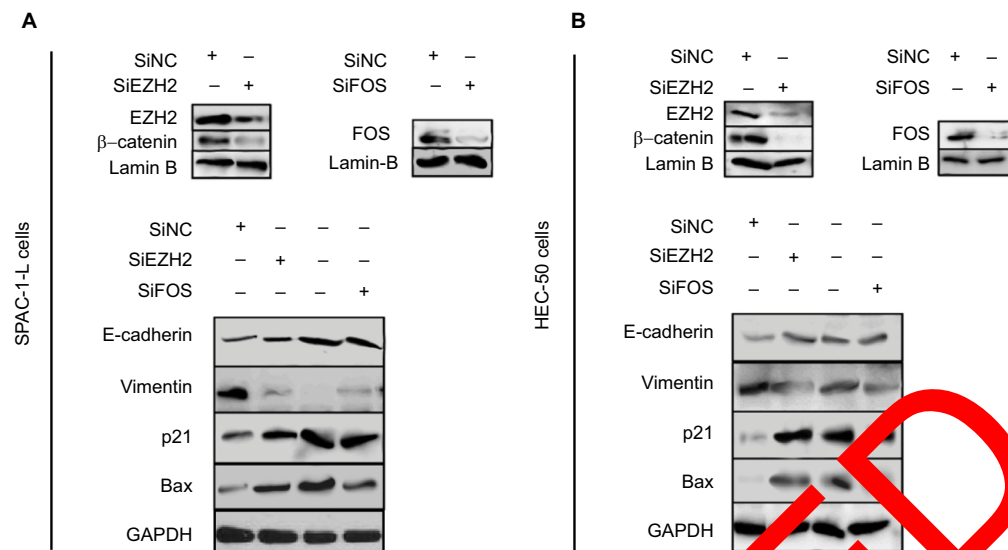


Figure 7 Western blot analysis of EZH2 and FOS in EC cells.

Note: (A, B) Results of Western blot analysis of EZH2 and FOS in SPAC-1-L and HEC-50 cells after transfer with siRNAs (siEZH2 and siFOS) or control siRNA (siNC).

Abbreviation: NC, negative control.

that the expression of miR-365 decreased in cancer tissues significantly compared to adjacent normal tissues (Figure 9A). The relative mRNA levels of EZH2 were highly significant in cancer tissues compared to normal tissues ($P < 0.001$). Similarly, the mRNA levels of FOS were also significantly higher compared to those in normal tissues ($P < 0.05$; Figure 9B). The outcomes of qRT-PCR suggested an inverse correlation between upregulation of FOS and EZH2 and knockdown of miR-365 (Figure 9C, D).

Immunohistochemistry staining was done in 40 cases of grade 3 endometrial EC for studying the levels of FOS and EZH2 (Figure 10E). Compared to sections of normal adjacent tissues, the cancerous endometrial tissues showed higher expression levels of FOS and EZH2, consistent with the results of in vitro experiments showing FOS and EZH2 as favorable targets of miR-365 in EC cells. The outcomes also suggested the miR-365 FOS/EZH2 signaling pathway as a potential mechanism underlying the aggressive EC tumor and metastasis, creating a potential therapeutic target.

Discussion

miRNAs are short noncoding RNAs responsible for silencing and regulating various genes, thus altering cellular processes and behaviors.⁴ The studies related to the functional roles and mechanisms involved for certain miRNAs could provide valuable data for designing new miRNA-influenced treatment

therapies. Studies till now suggest miR365 to show tumor suppressor or oncogenic activity in a number of cancers such as lung cancer,⁷ cutaneous squamous cell carcinoma,^{8,9} pancreatic cancer,¹⁰ gastric cancer,¹¹ breast cancer,¹² malignant melanoma, colon cancer, and ovarian cancer.^{13–15} Looking into the dual role of miR365 in various malignancies, its involvement in tumorigenesis and biological function in EC remains unexplored.

In the present investigation, we showed that levels of miR-365 were significantly suppressed in selected EC cells compared to immortalized human endometrial epithelial cells. We found that increase in the levels of miR-365 in EC cell lines resulted in decreased cell proliferation via apoptosis and senescence. Upregulation of miR-365 in cancer cells decreased cell migration and invasion, reconstructed paclitaxel sensitivity, and inhibited the formation of spheres. In the study, we further discovered the favorable targets of miR-365 using in silico prediction tools. We found that FOS and EZH2 served as direct targets of miR-365; hushing these target genes using siRNAs showed the tumor-suppressive effect of miR-365 overexpression in cancerous endometrial cells. Further, the results of qRT-PCR along with immunohistochemistry suggested that an inverse correlation existed between the levels of miR-365 and FOS and EZH2 in cancerous endometrial tissues. The findings of our study suggested that miR-365 plays an important role in malignant



Figure 8 Decrease in expression of *EZH2* and *FOS* suppresses invasion, proliferation and CSC-like phenotypes of cancerous endometrial cancer cells.

Notes: The results indicate the number of cells that underwent apoptosis, sphere formation assay, cells senescence, and invasion fold change in (A) SPAC-1-L and (B) HEC-50 cells after 72 hours of transfection. ** $P < 0.01$ compared to siRNA (si-NC).

Abbreviations: NC, negative control; SA-β-gal, senescence-associated β-galactosidase; TUNEL, terminal deoxynucleotidyl transferase mediated dUTP nick-end labeling.

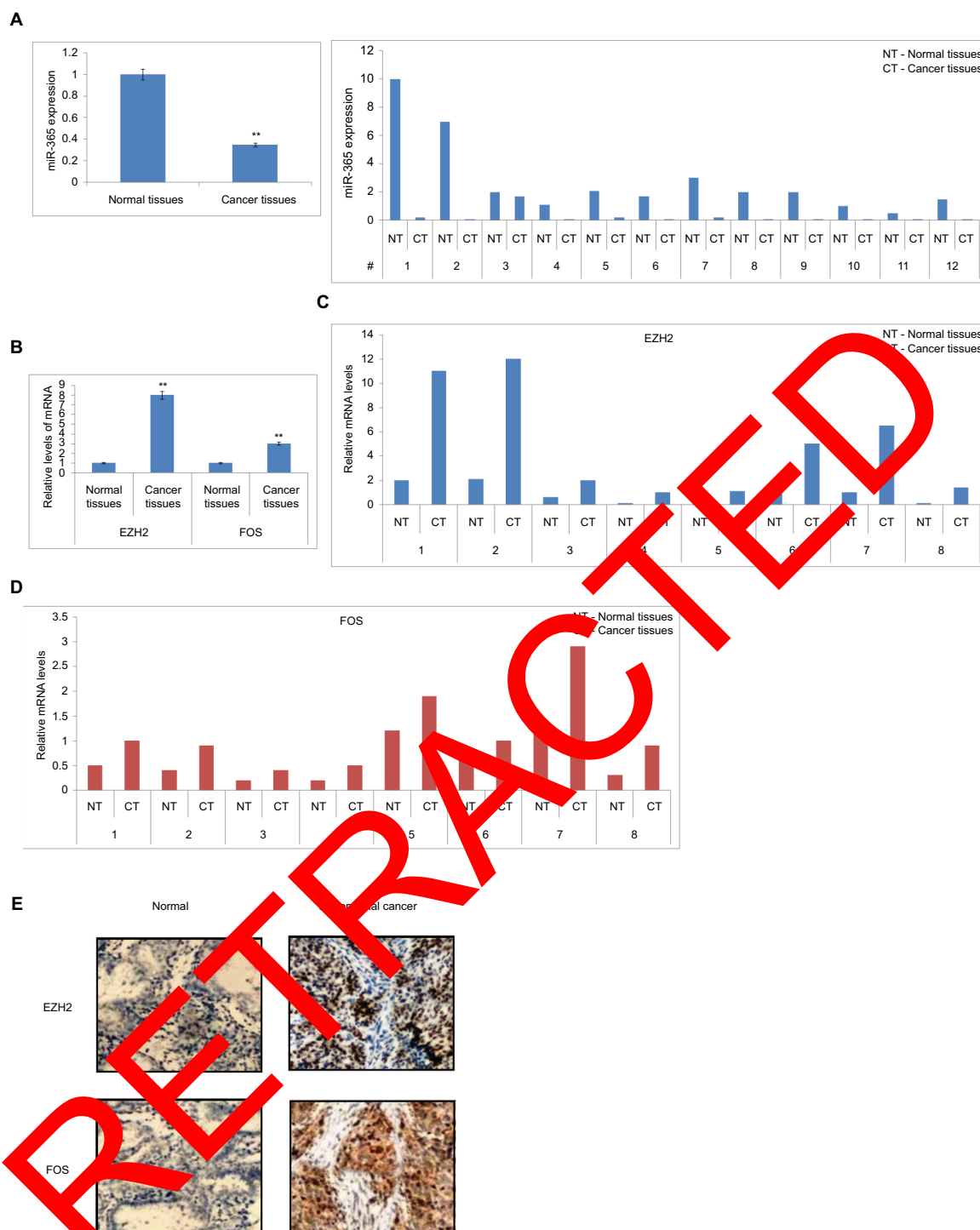


Figure 9 An inverse correlation existed between down-regulation of miR-365 and up-regulation of *EZH2* and *FOS* in endometrial cancer tissue.

Notes: (A) Results of qRT-PCR showed the suppression of miR-365 in 12 pairs of selected cancerous EC tissues (CT) and the normal tissues (NT) adjacent to them. (B–D) The qRT-PCR results of *EZH2* and *FOS* in eight pairs of EC, along with those of adjacent normal tissues. (E) Images after IHC analysis of *EZH2* and *FOS* in tissues of patients suggested elevated expression of *EZH2* and *FOS* in cancer cells and in cells reported to be benign. ** $P < 0.01$ compared to normal tissues.

Abbreviations: EC, endometrial cancer; IHC, immunohistochemistry; qRT-PCR, quantitative real-time reverse transcriptase-polymerase chain reaction.

phenotypes of cancer cells, such as cancer stemness, migration, proliferation, and invasion, via suppressing the levels of FOS and EZH2.

EZH2 has been reported to show potential role in development of cancer through its character to silence tumor suppressor genes.³³ A study concluded that overexpression of EZH2 is a representation of aggressive or advanced cancer in many human tumors.³⁴ The upregulation of EZH2 marks the presence of invasive phenotype in cancer cells via suppressing TIMP-3, which is a tumor suppressor.³⁵ Suppression of EZH2 in cancerous cells caused apoptosis, mesenchymal-to-epithelial transition, and cellular senescence;^{36,37} also, a study found that the activity of EZH2 is vital for CSC maintenance.³⁸

Findings till now have found a close link between overexpression of EZH2 and invasion of EC.^{39,40} The studies have suggested that inhibition of EZH2 expression in cancerous EC cells caused decrease in cell migration, invasion, and proliferation either by inactivating Wnt/ β -catenin signaling or by upregulating the levels of E-cadherin.⁴¹ The outcomes of our study suggested that miR-365 promoted senescence and apoptosis; in addition to this, it caused the suppression of EMT and CSC-like character of EC cells via modulating the expression levels of EZH2 along with elevating the levels of p21, Bax, and TIMP-3 and downregulating the levels of Wnt/ β -catenin (Figure 7A, B), the mesenchymal markers.

Along with EZH2, we found that miR-365 targeted FOS, which is reported to regulate both metastasis and tumorigenesis. FOS has been discovered to possess oncogenic property by promoting EMT.⁴² It has also been found to increase cell proliferation, invasiveness character, and the mobility of cancer cells.^{43,44} Besides this, the levels of FOS are higher in EC cells compared to normal cells, as suggested in a previous study.⁴⁵ A report suggested that silencing the activity of FOS in breast cancer cell lines caused upregulation of Bax and promoted apoptosis.⁴⁶ Contrary to this, it also showed tumor suppressor effect.⁴⁷ Hence, it is not clear about the negative regulation of FOS which leads to suppression of proliferation, CSC-like character, and invasion of EC cells by miR-365. In the present investigation, we demonstrated that suppression of FOS leads to senescence and apoptosis, inhibits cell invasion, and reduces sphere forming ability of the EC cells. Our study confirmed that miR-365 may affect multiple steps in the metastasis of EC cells via targeting EZH2 and FOS pathways.

Conclusion

We established that miR-365 inhibits growth, self-renewal, and invasiveness property of EC cells, simultaneously suppressing oncogenes such as EZH2 and FOS in EC. The

reports conclude that miR-365-EZH2/FOS pathway is the mechanism responsible for the invasiveness and stem cell-like character properties of EC cells. Therefore, the restoration of miR-365, or in combination with EZH2 and FOS inhibitors, could be a major therapeutic approach for halting the progression of EC.

Acknowledgment

This work was supported by grants from the National Natural Science Foundation of China (No. 31670844) and the science and technology innovation team support of universities in Henan (1717IRTSTHN021).

Disclosure

The authors report no conflicts of interest in this work.

References

1. Lujambio A, Lu J, SW. The microcosmos of cancer. *Nature*. 2012;482(7385):347–355.
2. Olivieri F, Rippo MR, Monsurro V, et al. MicroRNAs linking inflammation, cellular senescence and cancer. *Ageing Res Rev*. 2013;12(4):1056–1068.
3. Croce CM, Calin GA. miRNAs, cancer, and stem cell division. *Cell*. 2009;122(1):6–7.
4. Yan G, Gumireddy K, Li A, Huang Q. Regulation of mesenchymal phenotype by microRNAs in cancer. *Curr Cancer Drug Targets*. 2013;13(9):930–934.
5. Zhong X, Coukos G, Zhang L. miRNAs in human cancer. *Methods Mol Biol*. 2012;822:295–306.
6. Yanaihara N, Caplen N, Bowman E, et al. Unique microRNA molecular profiles in lung cancer diagnosis and prognosis. *Cancer Cell*. 2006;9(3):189–198.
7. Qi J, Rice SJ, Salzberg AC, et al. MiR-365 regulates lung cancer and developmental gene thyroid transcription factor 1. *Cell Cycle*. 2012;11(1):177–186.
8. Zhou M, Liu W, Ma S, et al. A novel onco-miR-365 induces cutaneous squamous cell carcinoma. *Carcinogenesis*. 2013;34(7):1653–1659.
9. Zhou M, Zhou L, Zheng L, et al. miR-365 promotes cutaneous squamous cell carcinoma (CSCC) through targeting nuclear factor I/B (NFIB). *PLoS One*. 2014;9(6):e100620.
10. Hamada S, Masamune A, Miura S, Satoh K, Shimosegawa T. MiR-365 induces gemcitabine resistance in pancreatic cancer cells by targeting the adaptor protein SHC1 and pro-apoptotic regulator BAX. *Cell Signal*. 2014;26(2):179–185.
11. Guo SL, Ye H, Teng Y, et al. Akt-p53-miR-365-cyclin D1/cdc25A axis contributes to gastric tumorigenesis induced by PTEN deficiency. *Nat Commun*. 2013;4:2544.
12. Zhang J, Zhang Z, Wang Q, Xing XJ, Zhao Y. Overexpression of microRNA-365 inhibits breast cancer cell growth and chemoresistance through GALNT4. *Eur Rev Med Pharmacol Sci*. 2016;20(22):4710–4718.
13. Bai J, Zhang Z, Li X, Liu H. MicroRNA-365 inhibits growth, invasion and metastasis of malignant melanoma by targeting NRP1 expression. *Cancer Biomark*. 2015;15(5):599–608.
14. Nie J, Liu L, Zheng W, et al. microRNA-365, down-regulated in colon cancer, inhibits cell cycle progression and promotes apoptosis of colon cancer cells by probably targeting cyclin D1 and Bcl-2. *Carcinogenesis*. 2012;33(1):220–225.
15. Wang Y, Xu C, Wang Y, Zhang X. MicroRNA-365 inhibits ovarian cancer progression by targeting Wnt5a. *Am J Cancer Res*. 2017;7(5):1096–1106.

16. Bokhman JV. Two pathogenetic types of endometrial carcinoma. *Gynecol Oncol.* 1983;15(1):10–17.
17. Gehrig PA, Bae-Jump VL. Promising novel therapies for the treatment of endometrial cancer. *Gynecol Oncol.* 2010;116(2):187–194.
18. Boren T, Xiong Y, Hakam A, et al. MicroRNAs and their target messenger RNAs associated with endometrial carcinogenesis. *Gynecol Oncol.* 2008;110(2):206–215.
19. Chung TK, Cheung TH, Huen NY, et al. Dysregulated microRNAs and their predicted targets associated with endometrioid endometrial adenocarcinoma in Hong Kong women. *Int J Cancer.* 2009;124(6):1358–1365.
20. Wu W, Lin Z, Zhuang Z, Liang X. Expression profile of mammalian microRNAs in endometrioid adenocarcinoma. *Eur J Cancer Prev.* 2009;18(1):50–55.
21. Dai Y, Xia W, Song T, et al. MicroRNA-200b is overexpressed in endometrial adenocarcinomas and enhances MMP2 activity by down-regulating TIMP2 in human endometrial cancer cell line HEC-1A cells. *Nucleic Acid Ther.* 2013;23(1):29–34.
22. Jiang F, Liu T, He Y, et al. MiR-125b promotes proliferation and migration of type II endometrial carcinoma cells through targeting TP53INP1 tumor suppressor in vitro and in vivo. *BMC Cancer.* 2011;11:425.
23. Hiroki E, Suzuki F, Akahira J, et al. MicroRNA-34b functions as a potential tumor suppressor in endometrial serous adenocarcinoma. *Int J Cancer.* 2012;131(4):E395–E404.
24. Dong P, Kaneuchi M, Watari H, et al. MicroRNA-194 inhibits epithelial to mesenchymal transition of endometrial cancer cells by targeting oncogene BMI-1. *Mol Cancer.* 2011;10:99.
25. Dong P, Kaneuchi M, Watari H, Sudo S, Sakuragi N. MicroRNA-106b modulates epithelial–mesenchymal transition by targeting TWIST1 in invasive endometrial cancer cell lines. *Mol Carcinog.* 2014;53(5):349–359.
26. Bai J, Zhang Z, Li X, Liu H. MicroRNA-365 inhibits growth, invasion and metastasis of malignant melanoma by targeting NRP1 expression. *Int J Clin Exp Pathol.* 2015;8(5):4913–4922.
27. Zhou L, Wang Y, Ou C, et al. microRNA-365-targeted nuclear factor I κ B transcriptionally represses cyclin-dependent kinase 6 and 4 to inhibit the progression of cutaneous squamous cell carcinoma. *Int J Biochem Cell Biol.* 2015;65:182–191.
28. Zhang P, Zheng C, Ye H, et al. MicroRNA-365 inhibits vascular smooth muscle cell proliferation through targeting cyclin D1. *Cell Mol Sci.* 2014;11(8):765–770.
29. Kim MH, Ham O, Lee SY, et al. MicroRNA-365 inhibits the proliferation of vascular smooth muscle cells by targeting cyclin D1. *J Cell Biochem.* 2014;115(10):1752–1761.
30. Zhou M, Liu W, Ma S, et al. A novel onco-miR-365 induces cutaneous squamous cell carcinoma. *Carcinogenesis.* 2014;34(7):1653–1659.
31. Dong P, Xu Z, Jia N, et al. Elevated expression of p53 gain-of-function mutation G75H in endometrial cancer cells can increase the invasive phenotypes and activation of the EGFR/PI3K/AKT pathway. *Mol Cancer.* 2013;12:105.
32. Dong P, Kaneuchi M, Xiong Y, et al. Identification of KLF17 as a novel epithelial–mesenchymal transition inducer via direct activation of TWIST1 in endometrioid endometrial cancer. *Carcinogenesis.* 2014;35(4):760–768.
33. Crea F, Fornaro L, Bocci G, et al. EZH2 inhibition: targeting the crossroad of tumor invasion and angiogenesis. *Cancer Metastasis Rev.* 2012;31(3–4):753–761.
34. Chase A, Cross NC. Aberrations of EZH2 in cancer. *Clin Cancer Res.* 2011;17(9):2613–2618.
35. Shin YJ, Kim JH. The role of EZH2 in the regulation of the activity of matrix metalloproteinases in prostate cancer cells. *PLoS One.* 2012;7(1):e30393.
36. Alimova I, Birks DK, Harris PS, et al. Inhibition of EZH2 suppresses self-renewal and induces radiation sensitivity in atypical rhabdoid teratoid tumor cells. *Neuro Oncol.* 2013;15(2):149–160.
37. Moore HM, Gonzalez ME, Toy KA, Cimino-Mathews A, Argani P, Kleer CG. EZH2 inhibition decreases p38 signaling and suppresses breast cancer motility and metastasis. *Breast Cancer Res Treat.* 2013;138(3):741–752.
38. van Vlerken LE, Kiefer CM, Morehouse C, et al. EZH2 is required for breast and pancreatic cancer stem cell maintenance and can be used as a functional cancer stem cell reporter. *Stem Cells Transl Med.* 2013;2(1):43–52.
39. Bachmann IM, Halvorsen OJ, Collett C, et al. EZH2 expression is associated with high proliferation rate and aggressive tumor subgroups in cutaneous melanoma and cancers of the endometrium, prostate, and breast. *J Clin Oncol.* 2013;31(2):268–277.
40. Zhou J, Ren W, Bandyopadhyay S, et al. Overexpression of enhancer of zeste homolog 2 (EZH2) and focal adhesion kinase (FAK) in high-grade endometrial carcinoma. *Gynecol Oncol.* 2013;128(2):344–348.
41. Eskander RN, Ji T, Huang B, Wardeh R, Randall LM, Hoang B. Inhibition of enhancer of zeste homolog 2 (EZH2) expression is associated with decreased tumor cell proliferation, migration, and invasion in endometrial cancer cell lines. *Int J Gynecol Cancer.* 2013;23(6):997–1005.
42. Kottmann AH, Schwarz H, Reichmann E, Oft M, Busslinger M, Beug H. The estrogen-dependent c-JunER protein causes a reversible loss of mammary epithelial cell polarity involving a destabilization of adherens junctions. *J Cell Biol.* 1996;132(6):1115–1132.
43. Eferl R, Wagner EF. AP-1: a double-edged sword in tumorigenesis. *Nat Rev Cancer.* 2003;3(11):859–868.
44. Li S, Fu H, Wang Y, et al. MicroRNA-101 regulates expression of the v-fos FBJ murine osteosarcoma viral oncogene homolog (FOS) oncogene in human hepatocellular carcinoma. *Hepatology.* 2009;49(4):1194–1202.
45. Fujimoto J, Hori M, Ichigo S, Morishita S, Tamaya T. Clinical implication of fos and jun expressions and protein kinase activity in endometrial cancers. *Eur J Gynaecol Oncol.* 1995;16(2):138–146.
46. Shi R, Peng H, Yuan X, et al. Down-regulation of c-fos by shRNA sensitizes adriamycin-resistant MCF-7/ADR cells to chemotherapeutic agents via P-glycoprotein inhibition and apoptosis augmentation. *J Cell Biochem.* 2013;114(8):1890–1900.
47. Teng CS. Protooncogenes as mediators of apoptosis. *Int Rev Cytol.* 2000;197:137–202.

Cancer Management and Research

Publish your work in this journal

Cancer Management and Research is an international, peer-reviewed open access journal focusing on cancer research and the optimal use of preventative and integrated treatment interventions to achieve improved outcomes, enhanced survival and quality of life for the cancer patient. The manuscript management system is completely online and includes

Submit your manuscript here: <https://www.dovepress.com/cancer-management-and-research-journal>

a very quick and fair peer-review system, which is all easy to use. Visit <http://www.dovepress.com/testimonials.php> to read real quotes from published authors.

Dovepress